journal

J. Am. Ceram. Soc., 96 [10] 3094–3099 (2013)
DOI: 10.1111/jace.12452

Combining Soft Chemistry and Spark Plasma Sintering to Produce Highly Dense and Finely Grained Soft Ferrimagnetic $Y_3Fe_5O_{12}$ (YIG) Ceramics

Thomas Gaudisson,[‡] Ulises Acevedo,[‡,§] Sophie Nowak,[‡] Nader Yaacoub,[¶] Jean-Marc Greneche,[¶] Souad Ammar,[‡] and Raul Valenzuela[§]

[‡]ITODYS, Université Paris Diderot, PRES Sorbonne Paris Cité, CNRS UMR-7086, Rue Jean-Antoine de Baïf, Paris 75205, France

[§]DMMC, Instituto de Investigaciones en Materiales, Universidad Nacional Autónoma de México, Ciudad de México 04510, México

[¶]LUNAM, Université du Maine, Institut des Molécules et Matériaux du Mans CNRS UMR-6283, Avenue Olivier Messiaen, Le Mans 72085, France

We report the synthesis of yttrium iron garnet (YIG) combining soft chemistry route, namely the polyol process, and spark plasma sintering (SPS) technique. The polyol process produced an intermediary amorphous phase containing both iron and yttrium cations in the desired ratio. They were annealed at 400°C in air to decompose the organic content of the reaction (polyol and acetate). To achieve the garnet phase, the polyol-obtained precursor was subjected to reactive SPS treatment at a temperature of 750°C, far below the typical temperatures (1350°C) used in the classic solid-state reaction process. In 15 min pure and high-density $Y_3Fe_5O_{12}$ ceramic, with about 100 nm sized crystalline grains, was obtained. We report as well the characterization of the initial amorphous phase and the obtained YIG by X-ray diffraction, scanning electron microscopy, Fourier-transform infrared spectroscopy, ^{57}Fe Mössbauer spectrometry, and magnetization measurements.

I. Introduction

The garnet structure (the mineral garnet is $Mn_3Al_2Si_3O_{12}$) is very stable,[1] with space group O^h10-$Ia3d$ and general formula $A_3B_5O_{12}$. In synthetic garnets with ferrimagnetic properties, A is generally a rare-earth cation, and B a transition-metal cation. The crystal structure is based on a polyhedral arrangement of oxygen anions defining three kinds of cation sites or sublattices, with dodecahedral (three sites per formula), octahedral (two sites per formula), and tetrahedral (three sites per formula) symmetry, respectively. The dodecahedral sites are normally occupied by the rare-earth cation (yttrium), while the transition 3*d* metals enter tetrahedral and octahedral sites. When the transition metal is iron (Fe^{3+}), there is a strong tendency to become ordered in an antiparallel magnetic arrangement. The magnetic moment of a rare-earth cation on dodecahedral sites adds to the octahedral iron's leading to a ferrimagnetic material. A particular advantage for applications is the fact that the garnet structure can form a large variety of total solid solutions, allowing the partial or total substitutions of many elements. In turn, this leads to the possibility of an extensive tailoring of magnetic properties.

Ferrimagnetic garnets have unique magneto-optical[1,2] and high-frequency properties, which have found original applications in a variety of devices. As yttrium iron garnet (YIG) exhibits the smallest linewidth for ferromagnetic resonance,[3] it is particularly considered for microwave devices. For all these applications, it is well-established that a high-density solid body is required instead of a powder.

Using the classic solid-state reaction methods,[1,2] a high-temperature reaction of about 1350°C is needed to achieve a garnet single phase. Less conventional routes have been also reported, such as co-precipitation,[4] sol–gel,[5,6] citrate gel,[7] plasma spraying,[8] pulsed laser ablation,[9] high-energy ball milling,[10] among others. Most of them require a subsequent annealing at more than 900°C–1000°C to obtain the crystalline phase[4,7–10] and in all the cases, a high-temperature sintering step is needed to achieve dense ceramic for the desired applications.

In this article, we describe the synthesis of YIG by means of the polyol process and then subsequent spark plasma sintering (SPS) treatment. Indeed, for such complex oxides, the polyol method provides a precursor which can be thermally annealed at very low temperatures as compared with the solid-state reaction to achieve the garnet crystal phase. SPS technique is mainly known to allow sintering of materials and multimaterials in a few minutes with a high compactness.[11] It is a nonconventional sintering technique based on the use of pulsed current, enabling fast heating rates and lower sintering temperatures in comparison with conventional sintering techniques.[12] It also appears recently that SPS is a new technique to achieve very fast solid-state chemistry.[13] Even though all the mechanisms are not well understood, it is generally agreed that an accelerated diffusion process due to the electrical discharge is at the origin of the fast reactivity by SPS.[14] SPS has been used for the consolidation of yttrium-aluminum garnets (YAG) allowing the preparation of carbon-free, full density samples with applications in optical transmittance devices,[15] ultrafine structured YAG-Al_2O_3,[16] and photoluminiscent YAG,[17] for instance. YIG has also been obtained from ball-milled reagent grade oxides subsequently sintered in SPS at temperatures in the 900°C–950°C range.[18]

The recovered intermediary solid phase from the heated polyol metal acetate solution appeared to be an amorphous hetero-metallic acetate–glycoxide where yttrium and iron cations are intimately mixed in the desired stoichiometric ratio (3:5). A subsequent annealing of the as-prepared powder at moderate temperature (400°C) is performed to decompose its main organic content, thus permitting to prevent any dramatic outgassing during SPS process. Finally, the

P. Joy—contributing editor

Manuscript No. 32020. Received September 15, 2012; approved May 7, 2013.
[†]Author to whom correspondence should be addressed. e-mail: ammarmer@univ-paris-diderot.fr

obtained residue was treated at 750°C under vacuum applying a static axial pressure of 100 MPa. A pure high-density $Y_3Fe_5O_{12}$ ceramic with crystalline grains of about 100 nm was thus obtained after 15 min. The final magnetic structure is confirmed by ^{57}Fe Mössbauer spectrometry and magnetic hysteresis measurements.

Other authors have also obtained YIG at low annealing temperatures.[19] Their procedure involves the coprecipitation from the corresponding nitrates, followed by evaporation to obtain a solid precursor. After annealing at temperatures in the 450°C–650°C range, the powders were digested[19] in a vessel, and the solid was recuperated by centrifugation, followed by vacuum evaporation and annealing again in the 450°C–650°C range to obtain the garnet phase. Final nanoparticle size was in the 9–25 nm range, depending on annealing temperatures.

II. Experimental Procedure

(1) Synthesis

Yttrium and iron acetates, $Y(CH_3CO_2)_3{\cdot}4H_2O$ and $Fe(CH_3CO_2)_2$, respectively, were dissolved in the stoichiometric ratio in diethyleneglycol. According to the classical procedure, the mixture was brought to the boiling point at a 6°C/min heating rate under mechanical stirring and maintained in reflux and stirring for 3 h.[20] After cooling down to room temperature, the precipitated solid was recuperated by centrifugation, washed with ethanol and dried in air at 50°C overnight.

The recovered powder was pretreated in air at 400°C for 2 h and subsequently used as starting material to form $Y_3Fe_5O_{12}$ phase by reactive SPS process. The precursor solid (typical batch of 1 g) is introduced into an Ø 8 mm carbon die with a layer of protective papyex. The system is closed by carbon punches at both sides which transmit the uniaxial pressure. DC pulses were delivered to the die by the punches using DR. SINTER515S SYNTEX SPS machine (Thiais, France) allowing the temperature to rise relatively slow (38°C/min) up to a first plateau of 400°C and rapidly (116°C/min) to a second one at 750°C. The soak time at 400°C does not exceed 5 min, with a pressure increasing from 50 to 100 MPa to avoid further dramatic outgassing, and that at 750°C with a constant pressure at 100 MPa for 15 min, and shorter heating time was also tested. The synthesis temperature and the thermal treatment were chosen based on the observation of the shrinkage versus the sample temperature. The time variation of the temperature (read on the left vertical axis) and that of the applied pressure (read on right vertical axis) are shown in Fig. 1(a). The shrinkage (contraction of the volume between the two graphite punches) is followed as a function of temperature in Fig. 1(b).

(2) Characterization

Powders and ceramics were characterized by X-ray diffraction (XRD) using a Panalytical XperPro equipped with a multichannel detector (X'celerator) using Co$K\alpha$ radiation (λ = 1.7889 Å) in the 10°–100° 2θ range and a scan step of 0.025 for 2 s. The diffractometer is also equipped with an Anton PAAR heating chamber no. HTK 1200N. Temperature resolved XRD patterns of the starting powder were thus recorded from 400°C to 900°C by a step of 50°C under inert atmosphere, namely ultra-pure N_2 (ALPHAGAZ 1000: AIR LIQUIDE Corp., Paris, France), for the same 2θ range. For all the crystallized phases, the cell parameter and the size of coherent diffraction domain (crystal size) were determined with the MAUD software, which is based on the Rietveld method combined with Fourier analysis.[21] Polycrystalline strain-free silicon was used as standard to quantify the instrumental broadening contribution.

The chemical composition of the produced powders and ceramics was checked by using an energy dispersive spectrometer (EDX) mounted on a JEOL-JSM (JEOL Ltd., France) 6100 scanning electron microscope (SEM) working between 20 and 35 kV. In a typical experiment the powder or a polished piece of the ceramic was directly sketched on a paper ahead of SEM/EDX analysis. Gold or Graphite was then sputtered on its surface to increase its conductivity.

Fourier transform infrared spectroscopy (FTIR) spectra of the as-produced and annealed powders were recorded with a Bruker Equinos spectrometer (Bruker, France) using the KBr pellet technique. They were obtained between 400 and 4000 cm^{-1} for 50 scans and a resolution of 4 cm^{-1}. On the as-produced powder, thermal analyses were performed with a Thermo Gravimetry/Differential Thermal Analyzer (TG/DTA) Setaram TGA92 apparatus (Setaram Instrumentation, Caluire, France) from room temperature up to 1000°C in air (20°C/min).

The microstructure of the produced ceramics was investigated by scanning electron microscopy using a Supra40 ZEISS (ZEISS, Germany) FEG-SEM microscope operating at 5.0 kV.

The ^{57}Fe Mossbauer spectra were recorded in a transmission geometry using ^{57}Co/Rh γ-ray source mounted on an electromagnetic drive with a triangular velocity form. The samples consist of a thin powdered layer containing 5 mg Fe/cm^2. The obtained spectra were analyzed by a least-square fitting method to Lorentzian functions. The isomer shift values (δ) are referred to that of α-Fe at 300 K.

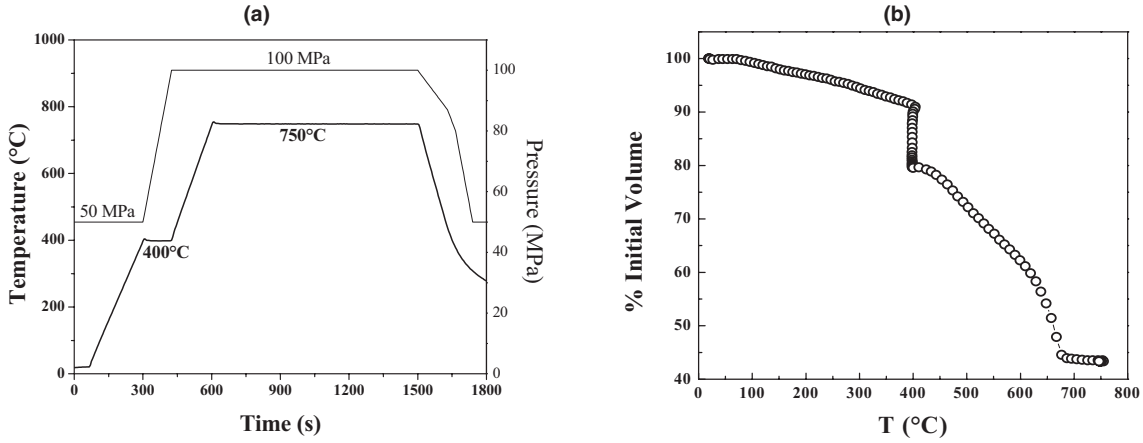

Fig. 1. Shrinkage curve in the SPS process of reactivity of $Y_3Fe_5O_{12}$: the sample temperature and pressure as a function of sintering time (a) and the initial sample volume ratio as a function of the temperature (b).

The 300 K-hysteresis loops were measured on a LDJ 9600 VSM magnetometer (LDJ ELECTRONICS, MD) with a maximum applied field of 10 kOe.

III. Results and Discussion

(1) Starting Powder

The XRD pattern of as-produced powder revealed an amorphous arrangement, in contrast with other oxides such as spinels, which can be directly synthesized by the polyol method to a high crystalline state. This can be attributable to the difference in structural complexity; the spinel unit cell is formed by 56 atoms, while the garnet unit cell needs 160 atoms (eight formula units). Due to such a complex structure, garnet precipitation requires high-temperature reaction, largely higher than those reached for spinel preparation in a polyol, typically the boiling temperature of common polyol solvent (diethyleneglycol has a boiling point of 245°C).

In this context, we proposed to first characterize exhaustively the as-produced precipitate to determine its intimate nature, and second to subsequently anneal it at different temperatures to monitor the formation of the garnet phase. Indeed, the polyol process has been widely used to prepare oxide materials where polyols, such as diethyleneglycol, can act as solvent and/or surfactant. Two-step polyol process is usually observed to synthesize metal oxide nanostructures. They involve first the preparation of a polyol-based metal alkoxide or an acetate-based metal hydroxide as intermediary phase[22,23] and (i) its *in situ* forced hydrolysis[22,23] or (ii) *ex situ* thermal decomposition.[24] The formation of the former compounds in liquid polyols is preceded by the dissolution of the precursor salt, generally acetates.

Clearly, due to its structural complexity, the preparation of garnet oxide proceeded through the route (ii) while that of spinel oxide may be easily achieved through the route (i).

To characterize the polyol-made amorphous solid phase, different experiments, including EDX spectrometry, FTIR spectroscopy and Thermogravimetry (TG) were carried out. EDX analysis showed that the as-produced powder mainly contains yttrium and iron atoms in the desired atomic ratio. Carbone and oxygen signals were also clearly evidenced on the recorded spectra. TG analysis showed that about 50% of the total molecular weight of the produced material departs (Fig. 2) between 200°C and 400°C, when heating in air. This suggests, in agreement with the EDX survey, that the as-produced amorphous intermediate solid is constituted by organic species mixed to inorganic cations, forming very probably a kind of hybrid framework, with a chemical composition very probably close to that of a hetero-metallic glycoxide or hydroxide, as observed elsewhere for metal oxide preparation using polyol process.[22–24] Note that the final solid decomposition product (after heating up to 1000°C) is the crystalline YIG phase. To distinguish between the hydroxide and glycoxide phases, IR transmission spectrum of

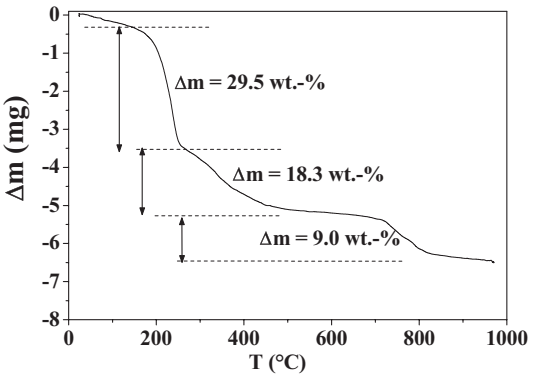

Fig. 2. TG thermogram of the as-produced solid precipitate in polyol, recorded in air with a heating rate of 20°C/min.

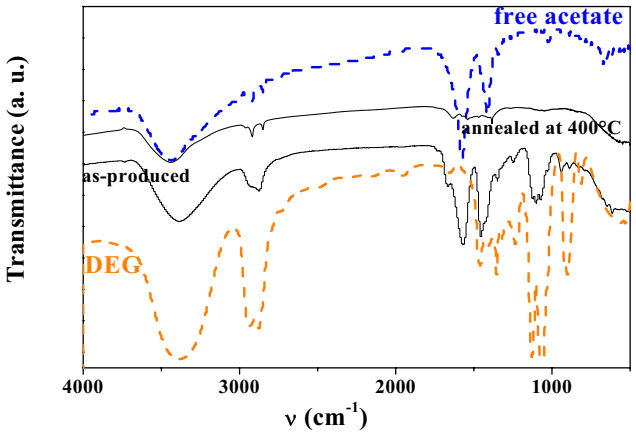

Fig. 3. FTIR spectra of the as-produced solid precipitate in polyol and its subsequently annealed at 400°C counterpart compared to those of free acetate and diethyleneglycol.

the as-produced powder was recorded and compared to those of free sodium acetate solid and diethyleneglycol liquid, respectively (Fig. 3). The analysis of the spectrum confirms the formation of a hybrid material. Indeed, it clearly shows the presence of (i) acetate ions, characterized by the specific symmetric and asymmetric ν(COO) vibration bands at 1573 and 1443 cm^{-1}, respectively,[25,26] and (ii) diethyleneglycol, characterized by the ν(OH) band at 3390 cm^{-1}, ν(CH_2) vibration bands at 2956–2875 cm^{-1}[25] and ν_s(C–O) bands at 1115–1065 cm^{-1}.[27]

An attentive inspection of the carboxylate vibration region shows that the difference $\Delta\nu = \nu_{as}(COO)–\nu_s(COO)$ is equal to 130 cm^{-1}. This value is usually attributed to ionic or bridging acetate.[27] Based on previous results, the bridging configuration remains the most probable. Indeed, in the case of zinc oxide, its formation in a polyol preceded by the formation of an *in situ* alkoxyacetate complex. Crystals were obtained in ethyleneglycol and diethyleneglycol and the structural resolution clearly showed that polyol and acetate anions complex the metal cations and that acetates act as bridges between these cations.[28]

Another observation may be made if one focuses on the hydroxyl stretching vibration zone. The intensity of ν(OH) band of the studied compound is significantly smaller than that of free diethylenegycol. It is most likely the result of polyol molecules partially deprotonated.

After annealing at 400°C the intensity of the FTIR peaks decreases significantly or disappears in agreement with the decomposition of the identified organic species and their departure.

Altogether, these results suggest the formation of coordination complexes where Y and Fe cations are coordinated to acetate and diethyleneglycol ligands, in a hetero-metallic acetate–glycoxide phase.

A careful examination of TG plot, evidenced a last weight loss (about 9 wt%) around 700°C, assumed to be due to carbonate departure. As a first approximation, one may suppose that carbonate species were formed during the decomposition of the organic part of the hybrid framework and re-adsorbed on the surface of the inorganic residue. Indeed, the infrared spectrum of the annealed polyol-made powder at 600°C (not shown) evidenced two very weak bands at 1558 and 1443 cm^{-1} attributed to residual organic species in relation to the exothermic decomposition of acetate and/or diethyleneglycol. They disapeared at 800°C. These bands may be assigned to reactive CO_2 adsorbed on metal oxide surfaces.[29]

Mössbauer experiments were performed on the as-prepared sample, to have additional information of the local cationic environment. As illustrated in Fig. 4, the Mössbauer spectra at 77 K exhibited quadrupolar structure with broad-

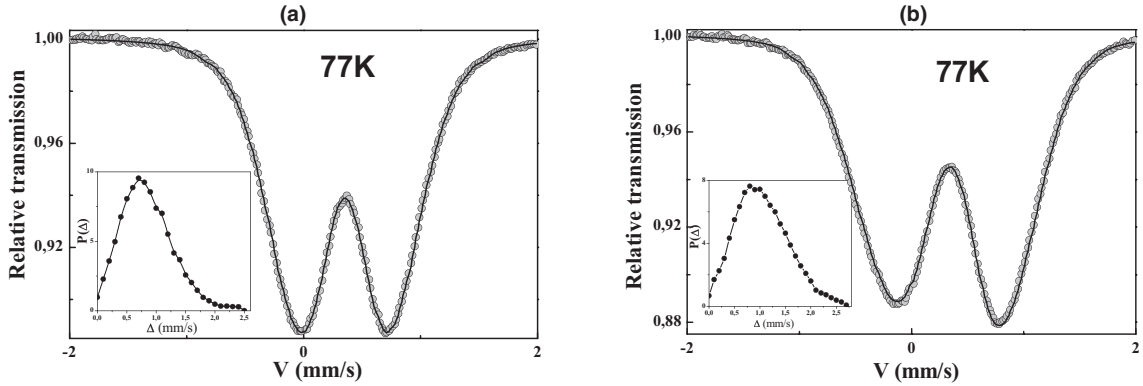

Fig. 4. 77 K-Mössbauer spectra of the as-produced solid precipitate in polyol (a) and of the subsequently annealed at 400°C counterpart (b), with their corresponding quadrupolar splitting distributions in respective insets.

Table I. Summary of Refined Values of Hyperfine Parameters Obtained at 300 and 77 K (Mean Isomer Shift <δ>, Mean Quadrupolar Shift <2εΔ, and Ratio $<\Delta^2>/<\Delta>^2$)

77 K	<δ> (mm/s) ±0.01	<2Δ > (mm/s) ±0.01	Ratio $<\Delta^2>/<\Delta>^2$ ±0.01
As-prepared	0.46	0.85	1.26
Annealed at 400°C	0.43	1.05	1.24

ened lines of similar intensities which can be described by means of a pure quadrupolar splitting distribution (see insets of Fig. 4). At 300 K (not shown here), similar features were observed on Mössbauer spectra. A more detailed analysis based on the mean isomer shift values (see Table I), the quadrupolar splitting distributions (see insets of Fig. 4) and ratio $<\Delta^2>/<\Delta>^2$ (parameter quantifying the topological disorder[30]) allows to conclude unambiguously that the material behaves as an amorphous containing octahedral Fe^{3+} (high-spin state) units while the mean hyperfine parameters remain much smaller than those estimated from amorphous bulk YIG samples.[7,31] When the as-prepared powders are annealed at 400°C, small changes appear in the quadrupolar doublets particularly due to the emergence of an asymmetry which does reflect the coexistence of both tetrahedral and octahedral Fe^{3+} units giving rise to a "new amorphous" state. The increase of the mean quadrupolar splitting gives rise to values rather consistent with those estimated on amorphous bulk garnets.[7,31]

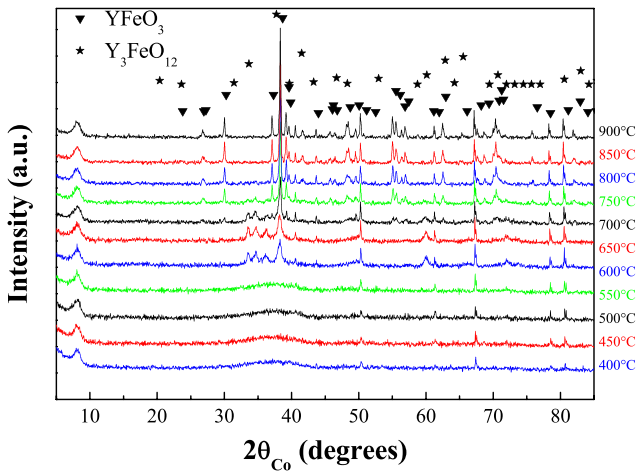

Fig. 5. Temperature resolved XRD patterns of the preannealed solid precipitate at 400°C. The temperature was increased by step of 50°C in a nitrogen atmosphere. Note that at 600°C the recorded pattern corresponds to that of orthoferrite $YFeO_3$ crystal structure, while at $T > 750$°C, they fit well with the garnet crystal structure.

With the aim of investigating the thermal conditions for the garnet structure formation starting from the preannealed at 400°C solid precipitate, a series of XRD patterns were measured as a function of temperature, as shown in Fig. 5. As can be seen, the $Y_3Fe_5O_{12}$ garnet appears for $T > 750$°C for simple annealing processes (not SPS). At lower temperatures, the orthoferrite phase, $YFeO_3$, is formed as an intermediate phase. We did not observe another crystalline phase, even if the Y/Fe ratio differs clearly from that expected in garnet phase. Very probably, the Y/Fe ratio is kept by the coexistence of an amorphous phase, a kind of carbonate, which decomposed between 700°C and 800°C forming $Y_3Fe_5O_{12}$. This transformation, coupled to the previously mentioned desorption processes, may be at the origin of the last weight loss (about 9%) observed during TG analysis.

(2) Sintered Ceramics

To obtain a solid dense pellet, we carried out sintering processes by means of the SPS method. This technique allows the application of large electric current pulses (up to 90 A) through the graphite crucible containing the powder while applying a high mechanical stress (up to 400 MPa). Extremely high heating and cooling rates can therefore be applied, which allows a fast sintering process at very low temperatures. Grain growth can be effectively prevented by this technique compared to the conventional sintering process at high temperatures (1350°C or more), which lead to an extremely rapid grain growth, thereby eliminating the novel properties of nanometric phases.

Applying the sintering conditions listed previously in the experiment section, different ceramics were produced at 750°C, varying the heating time at this temperature (from 5 to 15 min). The XRD pattern of sample sintered in SPS at 750°C for 15 min is presented in Fig. 6. The refined pattern using MAUD software shows unambiguously that only the YIG phase occurs for samples sintered under the mentioned conditions and the sharp lines indicate the well-crystalline state. The refined cell parameter [$a = 12.388(7)$ Å] agrees well with that of the stoichiometric bulk phase (JCPDS no. 00-043-0507). The crystallites appear to be strain free, almost isotropic in size with an average coherence length of 105 nm.

Note that the XRD pattern of the ceramics obtained with shorter heating time at 750°C exhibited traces of the orthoferrite phase, suggesting that the orthoferrite to garnet transformation required a minimum heating time of 15 min.

Scanning electron microscope analysis (Fig. 7) showed a highly dense and fine grained ceramic. The grains exhibit a typical polygonal shape with an average size of about 100 nm. The density of the produced ceramic was measured using the Arquimedes method, by weighing the sample in air and then in a liquid with a well-known density. The latter allows a determination of the volume. The obtained density was typically 4.84 g/cm^3, about 94% of the theoretical YIG value (5.17 g/cm^3).

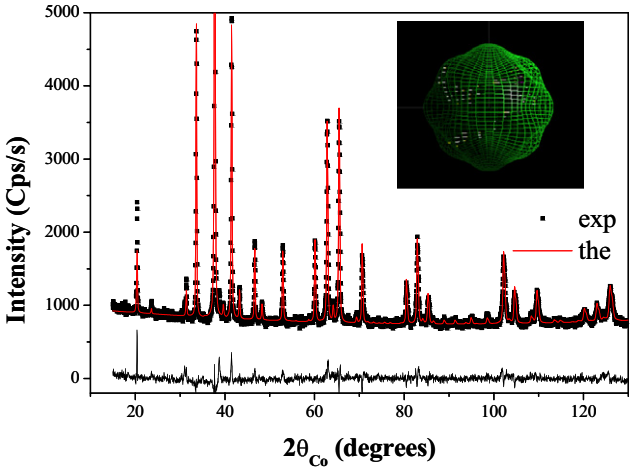

Fig. 6. The recorded (scatters) and calculated (continuous line) XRD patterns of the ceramics produced by SPS at 750°C for 15 min. The difference between the two patterns is given at the bottom of the figure. A representative morphology of the coherence domain of the studied ceramic, inferred from MAUD refinement, is given in the inset.

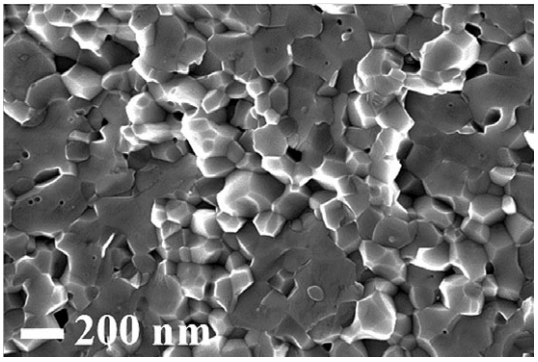

Fig. 7. Typical SEM images recorded on the ceramic produced by SPS at 750°C for 15 min.

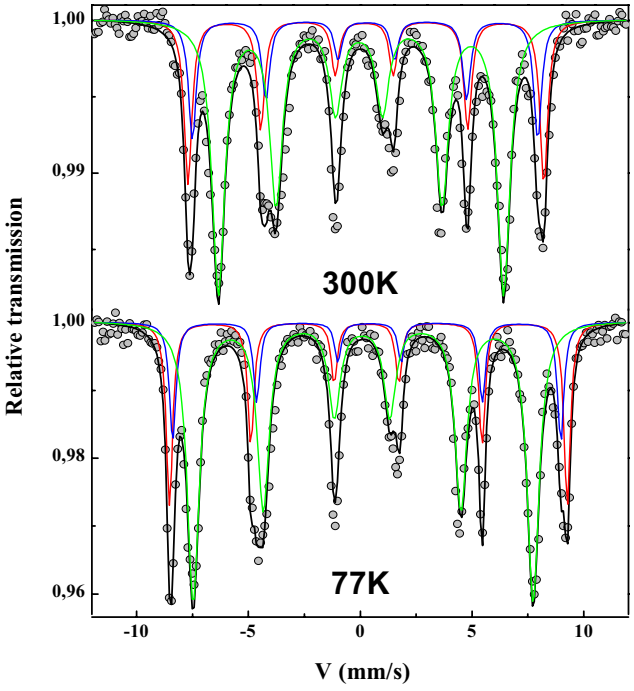

Fig. 8. 300 and 77 K Mössbauer spectra of the ceramic produced by SPS at 750°C for 15 min.

^{57}Fe Mössbauer experiments were performed on the ceramic obtained for 15 min SPS heating. The recorded spectra (Fig. 8) exhibit significant evolution of the hyperfine structure between this sample and the intermediate solids studied previously (see Fig. 4). Indeed, the 300 and 77 K Mössbauer spectra of this produced ceramic exhibited magnetic hyperfine structures, which consist of three components attributed to Fe^{3+} located in tetrahedral and octahedral sites, as discussed in.[32] The proportions and the respective hyperfine characteristics are highly consistent with those of crystalline bulk YIG systems prepared by conventional methods, that is, ceramic route [32] (see data listed in Table II).

The hysteresis loop of this sample was obtained at room temperature, as it appears in Fig. 9. The saturation magnetization, M_s = 26.6 emu/g, is in very good agreement with the bulk value reported for YIG (27.4 emu/g[33]). In YIG, as Y^{3+} is diamagnetic, the total magnetic moment in YIG is determined by the superexchange interactions between the three Fe^{3+} in tetrahedral sites and the two Fe^{3+} in octahedral sites (per formula), which leads to ~5 Bohr magnetons per formula at 0 K. By taking into account the unit cell parameter (12.386 Å) and a density of 5.17 g/cm^3, the magnetization value is 38.3 emu/g at 0 K. Thermal fluctuations decrease this value to 27.4 emu/g at room temperature. In the case of nanostructured YIG, lower values of M_s have been reported (M_s ~ 25 emu/g[34]). The coercive field appears higher than most reported (about 50 Oe for particles in the 1 μm range[34]), probably due to the nanosized dimensions of grains. A study on the dependence of coercive field as a function of synthesis parameters (and their effect on microstructure) would be very interesting, but it is beyond the scope of the

Table II. Summary of Refined Values of Hyperfine Parameters Obtained at 300 and 77 K (Isomer Shift δ, Quadrupolar Shift 2ε, Hyperfine Field B_{hyp}, and Ratio%). Comparison is Done with Data Listed in [32]

	δ (mm/s) ±0.01	2ε (mm/s) ±0.01	B_{hyp} (T) ±1	% ±2
300 K (O1)	0.38	0.08	49.2	23
(O2)	0.40	−0.05	47.7	16
(T)	0.15	0.09	39.3	61
77 K (O1)	0.48	0.09	55.0	22
(O2)	0.51	−0.13	53.6	15
(T)	0.26	0.05	46.9	63
300 K (O1)	0.39	0.08	49.7	28
(O2)	0.33	−0.03	48.0	12
(T)	0.16	0.01	39.8	61
4.2 K (O1)	0.47	0.13	56.1	23
(O2)	0.44	−0.01	54.3	16
(T)	0.25	0.00	47.5	61

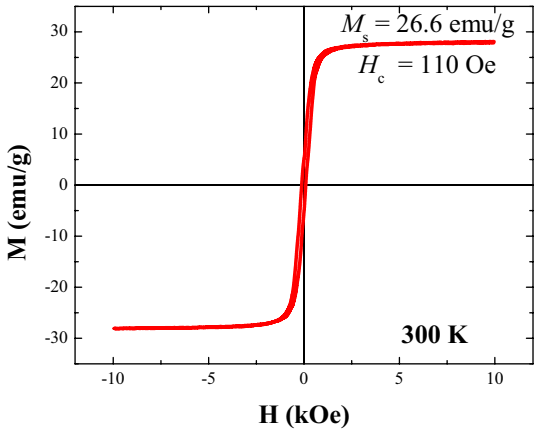

Fig. 9. 300 K magnetic hysteresis loops of the SPS-produced YIG.

present report. As a comparison, the magnetization values obtained for dispersed NPs obtained at similarly low-annealing temperatures[19] with a smaller size are considerably lower. Values as small as M_s = 7.5 emu/g were observed for NPs of 9 nm, increasing to 20.6 for NPs of 25 nm. We can estimate that the M_s value obtained in this study for the SPS sintered samples is very close to the bulk value because of two reasons: grains are larger (about 100 nm), and they have been consolidated as a polycrystalline body, which leads to additive magnetic interactions between grains.

IV. Conclusion

We have described the process to obtain nanostructured YIG by the forced hydrolysis of the metals in a polyol, followed by a SPS sintering at 750°C for 15 min. This combination of methods leads to significant less time and energy consuming processing, allows a single phase garnet structure with well-crystallized grains of about 100 nm in size, at temperatures 650°C below the typical solid-state sintering process, for sintering times as short as 15 min. The magnetic structure and properties of these ceramics are similar to those reported for the ferrimagnetic compounds prepared by ceramic route, opening thus real opportunity to use them for microwave devices.

Acknowledgments

Authors thank the technical contribution from Benjamin Villeroy (ICMPE, CNRS Thiais) for SPS experiments and Raul Ortega-Zempoalteca (IIM, UNAM, México) for VSM measurements. This study was partially supported by French-Mexican ANR MINAFC-CONACyT (Mexico) grant no. 139292.

References

[1]R. Valenzuela, *Magnetic Ceramics*. Cambridge University Press, Cambridge, 2005.

[2]M. Niyaifar Ramani, M. C. Radhakrishna, A. Hassnpour, M. Mozaffari, and J. Amighian, "Magnetic Studies of $Bi_xY_{3-x}Fe_5O_{12}$ Fabricated Using Conventional Method," *Hyperfine Interact*., **187** [1–3] 137–40 (2008).

[3]N. Mo, J. J. Green, B. A. Beitscher, and C. E. Patton, "High Precision-Metrology Based Microwave Effective Linewidth Measurement Technique," *Rev. Sci. Instrum*., **78** [1–3] 113903–11 (2007).

[4]M. M. Rashad, M. M. Hessien, A. El-Midany, and I. A. Ibrahim, "Effect of Synthesis Conditions on the Preparation of YIG Powders via co-Precipitation Method," *J. Magn. Magn. Mater*., **321** [22] 3752–7 (2009).

[5]Z. Cheng, H. Yang, L. Yu, and W. Xu, "Saturation Magnetic Properties of $Y_{3-x}Re_xFe_5O_{12}$ (Re: Gd, Dy, Nd, Sm and La) Nanoparticles Grown by a Sol-Gel Method," *J. Mater. Sci. - Mater. Electron*., **19** [5] 442–7 (2008).

[6]E. Garskaite, K. Gibson, A. Leleckaite, J. Glaser, D. Niznansky, A. Kareiva, and H. J. Meyer, "On the Synthesis and Characterization of Iron-Containing Garnets ($Y_3Fe_5O_{12}$, YIG and Fe_3Al_5IAG)," *Chem. Phys*., **323** [2–3] 204–10 (2006).

[7]P. Vaqueiro, M. A. López Quintela, J. Rivas, and J. M. Grenèche, "Annealing Dependence of Magnetic Properties of Yttrium Iron Garnet Prepared by Citrate Gel Process," *J. Magn. Magn. Mater*., **169** [1–2] 56–68 (1997).

[8]B. G. Ravi, A. S. Gandhi, X. Z. Guo, J. Margolies, and S. Sampath, "Liquid Precursor Plasma Spraying of Functional Materials: A Case Study for Yttrium Aluminum Garnet (YAG)," *J. Therm. Spray Technol*., **17** [1] 82–90 (2008).

[9]N. B. Ibrahim, C. Edwards, and S. B. Palmerm, "Pulsed Laser Ablation Deposition of Yttrium Iron Garnet and Cerium-Substituted YIG Films," *J. Magn. Magn. Mater*., **220** [2–3] 183–94 (2000).

[10]F. Sánchez-De Jesús, C. A. Cortés-Escobedo, R. Valenzuela, S. Ammar, and A. M. Bolarín-Miró, "Synthesis of $Y_3Fe_5O_{12}$ (YIG) Assisted by High-Energy Ball Milling," *Ceram. Int*., **38** [6] 5257–63 (2012).

[11]R. Orru, R. Lichen, A. M. Locci, and G. Cao, "Consolidation/Synthesis of Materials by Electric Current Activated/Assisted Sintering," *Mater. Sci. Eng., R*, **63** [4–6] 127–287 (2009).

[12]J. Galy, M. Dollé, T. Hungria, P. Rozier, and J. P. Monchoux, "A New Way to Make Solid State Chemistry: Spark Plasma Synthesis of Copper or Silver Vanadium Oxide Bronzes," *Solid State Sci*., **10** [8] 976–81 (2008).

[13]Y. Regaieg, G. Delaizir, F. Herbst, L. Sicard, J. Monnier, D. Montero, B. Villeroy, S. Ammar-Merah, A. Cheikhrouhou, C. Godart, and M. Koubaa, "Fast Reactivity by Spark Plasma Sintering: The Case of Orthorhombic $LaMnO_3$ Compound," *Mater. Lett*., **80**, 195–8 (2012).

[14]Z. A. Munir, U. Anselmi-Tamburini, and M. Ohyanagi, "The Effect of Electric Field and Pressure on the Synthesis and Consolidation of Materials: A Review of the Spark Plasma Sintering Method," *J. Mater. Sci*., **41** [3] 763–77 (2006).

[15]N. Frage, S. Kalabukhov, N. Sverdlov, V. Ezersky, and M. P. Dariel, "Densification of Transparent Yttrium Aluminium Garnet (YAG) by SPS Processing," *J. Eur. Ceram. Soc*., **30** [16] 3331–7 (2010).

[16]Y. Harada, N. Uekawa, and T. Kojima, "Fabrication of $Y_3Al_5O_{12}$–Al_2O_3 Eutectic Materials Having Ultrafine Microstructure," *J. Eur. Ceram. Soc*., **28** [1] 235–40 (2008).

[17]E. H. Penilla, Y. Kodera, and J. E. Garay, "Simultaneous Synthesis and Densification of Transparent, Photoluminiscent Polycrystalline YAG by Current Activated Pressure Assisted Densification (CAPAD)," *Mater. Sci. Eng., B*, **177** [14] 1728–87 (2012).

[18]L. Fernandez-Garcia, M. Suarez, and J. L. Menendez, "Low Temperature Spark Plasma Sintering of YIG Powders," *J. Alloy. Compd*., **502** [1] 132–5 (2010).

[19]M. Rajendran, S. Deka, P. A. Joy, and A. K. Bhattacharya, "Size-Dependent Magnetic Properties of Nanocrystalline Yttrium Iron Garnet Powders," *J. Magn. Magn. Mater*., **301** [1] 212–9 (2006).

[20]Z. Beji, L. S. Smiri, N. Yaacoub, J. M. Greneche, N. Menguy, S. Ammar, and F. Fievet, "Heating Effect on the Magnetic Properties of Polyol-Made $Ni_{1-x}Zn_xFe_2O_4$ Nanocrystalline Powders," *Chem. Mater*., **22** [4] 1350–66 (2010).

[21]L. Lutterotti, S. Matthies, and H. R. Wenk, "MAUD: A Friendly Java Program for Material Analysis Using Diffraction," *IUCr: Newsletter of the CPD*, **21**, 14–5 (1999).

[22]L. Poul, "Oxydes et Hydroxyacétates Lamellaires de Métaux de Transition (Zinc, Cobalt, Nickel): Nouvelle Voie de Synthèse en Milieu Polyol, Caractérisation"; Ph.D thesis, Université Pierre et Marie Curie, Paris, 2000.

[23]L. Poul, S. Ammar, N. Jouini, F. Fiévet, and F. Villain, "Metastable Solid Solutions in the System ZnO–CoO: Synthesis by Hydrolysis in Polyol Medium and Study of the Morphological Characteristics," *Solid State Sci*., **3** [1] 31–42 (2001).

[24]D. Larcher, G. Sudant, R. Patrice, and J. M. Tarascon, "Some Insights on the Use of Polyols-Based Metal Alkoxides Powders as Precursors for Tailored Metal-Oxides Particles," *Chem. Mater*., **15** [18] 3543–51 (2003).

[25]L. Poul, N. Jouini, and F. Fiévet, "Layered Hydroxide Metal Acetates (Metal = Zinc, Cobalt, and Nickel): Elaboration via Hydrolysis in Polyol Medium and Comparative Study," *Chem. Mater*., **12** [10] 3123–32 (2000).

[26]K. Nakamoto, *Infrared and Raman Spectra of Inorganic and Coordination Compounds*. 4th Edition, John Wiley and Sons, New-York, 1986.

[27]D. Knetsch and W. L. Groeneveld, "Alcohol as Ligands. III. Complexes of Ethylene Glycol with Some Divalent Metal Halides," *Inorg. Chim. Acta*, **7** [1] 81–7 (1973).

[28]L. Poul, N. Jouini, F. Fiévet, and P. Herson, "A new two-Dimensional Alkoxyacetate of Zinc: Structure of μ-Acetato-μ-[Ethane-1,2-Olato(−1)]-Diacetatodizinc," *Z. Kristallogr*., **213** [78] 416–8 (1998).

[29]G. Busca and V. Lorenzelli, "Infrared Spectroscopic Identification of Species Arising From Reactive Adsorption of Carbon Oxides on Metal Oxide Surfaces," *Mater. Chem*., **7** [1] 89–126 (1982).

[30]M. E. López-Herrera, J. M. Grenèche, and F. Varret, "Analysis of the Mössbauer Quadrupole Spectra of Some Amorphous Fluorides," *Phys. Rev. B: Condens. Matter*, **28** [9] 4944–8 (1982).

[31]M. Toulemonde, G. Fuchs, N. Nguyen, F. Studer, and D. Groult, "Damage Processes and Magnetic Field Orientation in Ferrimagnetic Oxides $Y_3Fe_5O_{12}$ and $BaFe_{12}O_{19}$ Irradiated by High-Energy Heavy Ions: A Mössbauer Study," *Phys. Rev. B: Condens. Matter*, **35** [13] 6560–9 (1987).

[32]J. M. Greneche, H. Pascard, and J. R. Regnard, "Modification of $[FeO_4]$ Tetrahedral Site Number Induced by Fast-Neutron Irradiation in $Y_3Fe_5O_{12}$ Investigated by Mössbauer Spectroscopy," *Solid State Commun*., **65** [7] 713–7 (1988).

[33]A. J. Moulson and J. M. Herbert, *Electroceramics*. Chapman and Hall, London, 1990.

[34]X. Z. Guo, B. G. Ravi, P. S. Devi, J. C. Hanson, J. Margolies, R. J. Gambino, J. B. Parise, and S. Sampath, "Synthesis of Yttrium Iron Garnet (YIG) by Citrate-Nitrate Gel Combustion and Precursor Plasma Spray Process," *J. Magn. Magn. Mater*., **295** [2] 145–54 (2005). □